Renewable Energy 125 (2018) 472–484

Contents lists available at ScienceDirect

Renewable Energy

journal homepage: www.elsevier.com/locate/renene

Resolution of the cloud enhancement problem for one-minute diffuse radiation prediction

Allan R. Starke [a, *], Leonardo F.L. Lemos [a], John Boland [b], José M. Cardemil [c], Sergio Colle [a]

[a] LEPTEN - Laboratory of Energy Conversion Engineering and Energy Technology, Department of Mechanical Engineering, Federal University of Santa Catarina (UFSC), Florianópolis, Santa Catarina, Brazil
[b] Centre for Industrial and Applied Mathematics, University of South Australia, Mawson Lakes Boulevard, Mawson Lakes, SA, 5095, Australia
[c] Mechanical Engineering Department, Universidad de Chile, Beauchef 851, Santiago, Chile

ARTICLE INFO

Article history:
Received 11 August 2017
Received in revised form
20 February 2018
Accepted 22 February 2018
Available online 23 February 2018

Keywords:
Minute global
Diffuse and direct irradiance
BRL model
Irradiance separation models
Cloud enhancement

ABSTRACT

For design and simulation of solar energy systems, quality information about all components of solar irradiance is crucial. In cases when only global irradiance measurements are available, separation models are a useful method to estimate DNI and diffuse irradiation. Several of such models have been developed since the 1960s, most of them aiming to deliver estimates in hourly resolution. For higher data resolution, such as in minute data, those models are not able to describe fast transient and cloud enhancement phenomena commonly observed in data with smaller time-steps. This paper proposes an adaptation of the BRL separation model, making it capable of delivering more precise irradiance estimates for higher resolution data. Two models result from this adaptation: one for Brazil and other for Australia. The proposed models yield a more precise DNI and diffuse fraction estimates to their respective countries, compared to other separation models commonly used in the technical literature. For example, using the recommended Combined Performance Index *(CPI)* as a single statistical indicator, the proposed model yields DNI estimates with *CPI* from 230 to 350% for Australia, and from 270 to 800% for Brazil, while the Engerer model, recently recommended as a "quasi-universal" 1-min separation model, yields DNI estimates with *CPI* from 500 to 700% for Australia, and from 600 to 1800% for Brazil.

1. Introduction

Accurate information about the three components of solar irradiance – global horizontal irradiance (GHI), diffuse horizontal irradiance (DIF) and direct normal irradiance (DNI) – is fundamental for the correct design and performance assessment of solar energy systems. For instance, designing flat-plate solar collectors or fixed PV systems requires information of the global tilted irradiance (GTI) incident on the array plane, which is estimated from the values of the irradiance components. On the other hand, only the direct irradiance can be concentrated, therefore DNI results are essential for the assessment of concentrating solar power (CSP) and concentrating PV (CPV) systems. Nonetheless, the measurement of the three components at the same time (GHI, DNI and DIF) is expensive, since it requires complex tracking devices and significant operational efforts. As a result, the data is not always available, and in some cases the measurements are commonly incomplete due to equipment malfunctions or poor maintenance. To illustrate this scenario, Brazil has an extensive radiation measurement network, operated by the National Institute of Meteorology (INMET) [1], which comprises approximately seven hundred stations measuring only global solar irradiance. In contrast, the Brazilian Environmental Data Organization System (SONDA) [2] has only seventeen stations measuring the three irradiance components [3].

A common approach to overcome the lack of reliable information is using some sort of separation model to estimate both diffuse and direct components from global irradiance observations. Even in locations where no irradiance measurements are available, it is possible to consider satellite imagery and semi-physical models [4,5] to estimate GHI, and then apply a separation model to estimate the other two components [6].

The need for an accurate assessment of the three irradiance components is crucial for sizing and selecting solar energy technologies and applications, necessitating an ongoing pursuit of precise separation models. The separation models for irradiance

* Corresponding author.
E-mail address: allan.starke@lepten.ufsc.br (A.R. Starke).

https://doi.org/10.1016/j.renene.2018.02.107
0960-1481/

components were initially developed in the 1960s by Liu & Jordan [7], and since then hundreds of models have been proposed in the literature. Those models are derived from locally-measured data from different stations; different climatic conditions; modelling different temporal resolutions (e.g.monthly daily, hourly, minute); and considering one or several input variables (predictors) [8]. Moreover, these models consider different kinds of equations, most of them using linear piece-wise equations [9,10]; polynomial piece-wise equations [11]; quasi-physical models [12]; artificial neural networks [13]; and more recent studies use simple logistical relationships [14–17]; while other studies consider more complex approaches using machine learning techniques to combine different separations models [8].

Recently, Gueymard and Ruiz-Arias [6] reported an extensive validation study in which they tested 140 separation models considering the radiation data from 54 research-class stations from the Baseline Surface Radiation Network - BSRN. The authors employed high quality 1-min data of global and direct irradiance to assess the performance of these separation models for 1-min DNI predictions. They found that cloud enhancement and high-albedo effects intensify the errors in irradiance measurement. Usually, models that consider variability and clear-sky irradiance as predictors tend to perform better. Most models overestimate DNI in cases when the solar intensity increases, caused by scattered irradiance from nearby clouds, commonly denominated as cloud enhancements events. The exceptions are the Engerer2 [17] and Perez2 [4] models, which tend to underestimate the DNI in a small degree in those events. Gueymard and Ruiz-Arias recommend 9 models as candidates for providing accurate and consistent results; Engerer2, Perez2, Boland5, Engerer1, Hollands2, Perez1, Perez3, Skartveit1 and Yao2 (according to the nomenclature defined by Gueymard and Ruiz-Arias). As discussed in Ref. [6], the success of the Engerer2 model is probably because this model was derived from 1-min data, thus allowing it to predict fast transient phenomena, such as cloud enhancements.

Based on the information gathered in recent studies [6,18,19], hourly separation models are not enough to meet the current demands of the industry, since they are not able to appropriately describe fast transient episodes. In addition, the temporal resolution of solar radiation data has considerably improved, since modern radiometric stations are able to provide it in intervals ranging from 1 to 10-min. Moreover, to reduce the economic uncertainty and improve the economic attractiveness of solar energy systems, the energy simulation programs should consider solar radiation databases with time-steps significantly shorter than 1 h (as in standard TMY databases). For instance, CSP plants present non-linear and transient effects that are substantially affected by the temporal resolution of the solar data, meaning 10-min or less is the ideal time step for simulating these kind of systems [20,21]. For PV applications, the temporal resolution requirements are even more stringent, since the effects caused by cloud enhancement are being studied at a time step of 3-s [19,22,23].

Hence, our main motivation is to develop a new separation model valid for 1-min irradiation data (global, diffuse and direct), and able to capture transient effects of irradiance, such as cloud enhancement. Modelling cloud enhancement in a separation model is not new, it was first introduced in Ref. [24], where the author proposed a separation model based in a generalized logistic function, and considering a new predictor and a linear correction to account the cloud enhancement events. This new predictor contemplates the deviation between the clearness index and the clear index of a clear-sky, while the linear correction is an offset term based on the ratio between actual and clear-sky global horizontal irradiance. The Ref. [24] model was recommended by Gueymard and Ruiz-Arias [6] as one of the most accurate models, its success is probably because it was derived from 1-min data. Based on the poor results of Engerer model for Brazil and to a certain extent for Australia when considering indicators of distribution similitude, it is most likely that the linear correction used by Engerer to account the cloud enhancements events is not enough to model this phenomenon.

Therefore, the main goal of this study is to derive a separation model, based on a logistical function using 1-min global, diffuse and direct irradiance data. The model should be able to capture transient effects of irradiance, providing accurate and consistent results. The choice of a logistical function is based on the recent achievements of this kind of models [15,16,24], comprising an exceptional performance, and a much simpler approach than other models. However, the sigmoidal shape of the logistical function makes impossible for the BRL model to capture the cloud enhancement events, *i.e.* the increase in the diffuse fraction for clearness index higher than 0.8. To overcome this, we propose to add modelled clear-sky irradiance (CSI) as a predictor and use a piecewise function. The intervals of the function's domain are defined by the ratio between global horizontal and global clear-sky irradiances. For the sake of simplicity, the same logistical equation is used in both sub-domains. To assess the performance of this new model a formal error analysis is performed, based on comparisons between our work and the models of Ridley [15], Engerer [24], Skartveit et al. [25] and Perez et al. [4].

The BRL separation model [15] (Ridley2) is adopted as basis for the model proposed herein, but introducing modifications to consider the phenomena related to fast transients. The choice for the BRL (Ridley2) [15] model instead of Boland5 [16] (as originally suggested in Ref. [6]), is due to two reasons. The first one is that the Boland5 model [16] shows that the use of a logistical model for directly calculating DNI from GHI provides marginal differences between DNI values calculated using diffuse fraction estimates from the (BRL) Ridley2 model. The second reason is our preference for using the classical approach of developing a model to calculate the diffuse fraction (d = DIFF/GHI), and then calculating the DNI from the relation (DNI = (1-d)GHI/sin α).

2. BRL logistic model for minute irradiance

Boland et al. [26] demonstrated with statistical rigour the usefulness of employing a logistical instead of piecewise linear or simple nonlinear functions for modelling diffuse fraction. Afterwards, Ridley et al. [15] proposed the generic multiple predictor logistic model, known as the Boland–Ridley–Lauret (BRL) model, given by,

$$\widehat{d} = \frac{1}{1 + e^{(\beta_0+\beta_1 k_T+\beta_2 AST+\beta_3\alpha+\beta_4 K_T+\beta_5\psi)}} = \frac{1}{1 + e^{(-5.38+6.63k_T+0.006AST-0.007\alpha+1.75K_T+1.31\psi)}} \quad (1)$$

where $\widehat{d}$ is the modelled diffuse fraction, k_T is the hourly clearness index, defined as the ratio of the global irradiance on a horizontal surface (I_g) to the extraterrestrial irradiance at the top of the atmosphere (I_0), also on a horizontal surface. *AST* is the apparent solar time, α is the solar altitude, K_T is the daily clearness index, and ψ is a persistence factor defined in Ref. [15]. The numerical values of the coefficients ($\beta_0, \beta_1, \ldots, \beta_5$) in Equation (1) are also derived in Ref. [15] using data from three meteorological stations in the southern hemisphere and four in the northern hemisphere. This model aims to use a minimum of measured variables; therefore, all the predictors can easily be calculated by well-known functions of solar geometry [27] (i.e. apparent solar time (*AST*), solar altitude (α), extraterestrial irradiance), and measurements of global, direct and

diffuse irradiance (to calculate clearness index, daily clearness index and persistence factor).

Fig. 1a depicts the relationship between diffuse fraction and clearness index (k_T). Four regions are observed in the d-k_T envelop, there are overcast, partly cloudy, clear-sky and cloud enhancements conditions. It can be seen that the overcast and clear-sky regions have a significant larger concentration of data points, being followed by the partly cloudy region. However, the cloud enhancement region has as many occurrences as partly cloudy, showing that this phenomenon should be considered in analysis of 1-min irradiance data. Additionally, Fig. 1b depicts the d-k_T envelope for Florianopolis (Brazil), as well as the diffuse fraction estimated by the BRL model. It is observed that the logistical form of BRL model captures the shape of the envelope for values for k_T close to 0.8. For higher values of k_T, the BRL model underestimates the diffuse fraction in the region characterised by the cloud enhancement phenomena.

Although the sigmoidal shape of the BRL model can't completely capture the shape of 1-min data, Lemos et al. [3] demonstrated that the BRL model is able to capture the larger spread of data observed in 1-min measurements, and properly fit the data if the cloud enhancements events are removed using estimations of clear-sky irradiance. That approach allowed the researchers to validate the usefulness of the model and extend its applications for modelling solar irradiance in shorter time-steps.

In order to predict the phenomena observed in 1-min data, a piecewise logistical function is proposed, where the domain break point is defined by the parameter K_{CSI}, which is defined as the ratio of the global horizontal irradiance (GHI) and global clear-sky irradiance (CSI). Therefore, it is possible to separate the model accounting for cloud enhancement events as a particular case. Moreover, the global clear-sky irradiance is added as a predictor because, as pointed out in Ref. [6], the models that take into account this parameter are in better agreement with experimental data. Thus, the diffuse fraction estimated by BRL-minute model is given by,

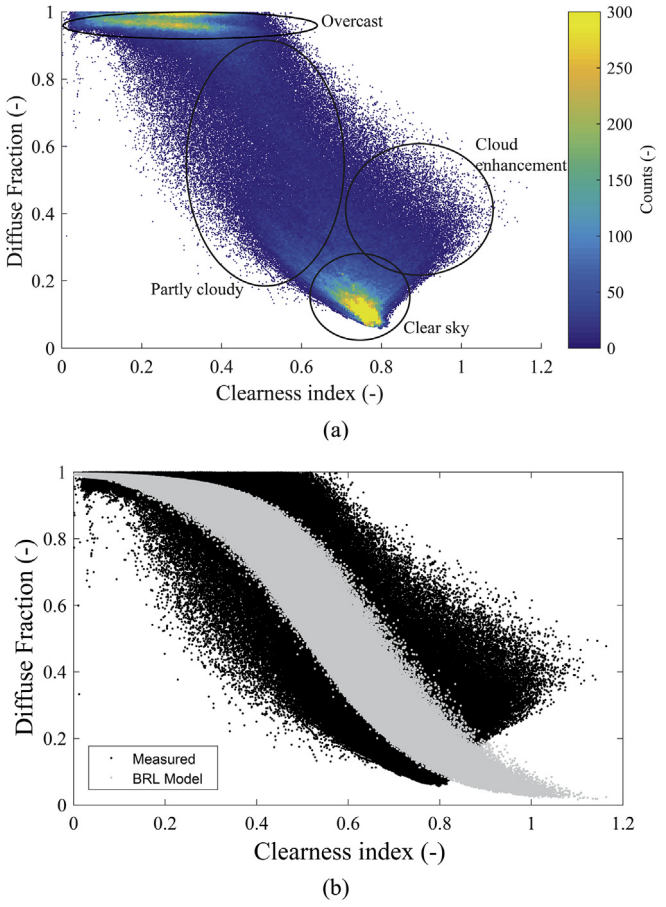

Fig. 1. Observed d-k_T envelop of 1-min irradiance data from Florianopolis – Brazil; (a) the colormap denotes the density of points (counts number). Four regions are highlighted: overcast, partly cloudy, clear-sky and cloud enhancements events; (b) overlaid with BRL generic multiple predictor logistical model.

$$\widehat{d} = \begin{cases} \dfrac{1}{1+e^{(\beta_0+\beta_1 k_T+\beta_2 AST+\beta_3\alpha+\beta_4 K_T+\beta_5\psi+\beta_6 CSI)}}, & K_{CSI} < 1.05 \\ \dfrac{1}{1+e^{(\beta_7+\beta_8 k_T+\beta_9 AST+\beta_{10}\alpha+\beta_{11} K_T+\beta_{12}\psi+\beta_{13} CSI)}}, & K_{CSI} \geq 1.05 \text{ and } k_T > 0.65 \end{cases} \quad (2)$$

where $\widehat{d}$ is the modelled diffuse fraction, from the new model, k_T is the hourly clearness index, AST is the apparent solar time, α is the solar altitude, K_T is the daily clearness index, and ψ is the persistence factor, CSI is the clear-sky irradiance and K_{CSI} is defined as the ratio of the measured global horizontal irradiance (GHI) and the modelled global clear-sky irradiance (CSI). The numeric values of the coefficients $(\beta_0, \beta_1, \ldots, \beta_{13})$ in Equation (2) will be derived using irradiance data from eight meteorological stations.

The choice of using K_{CSI} for splitting the sub-domains is due to its clear and intuitive interpretation, since values higher than unity means cloud enhancement events (CEE). The numerical value of 1.05 is established to avoid misleading classification, since clear-sky models have some approximation errors and can underestimate the clear-sky values. Clearness index higher than 0.65 $(k_T > 0.65)$ is considered to ensure that the second function does not affect non-cloud enhancement events. Both values (1.05 and 0.65) are chosen because of their physical significance: (i) GHI higher than CSI, (ii) physical impossibility of existence of CEE for clearness index lower than 0.65. Hence, this value is a conservative one, in comparison to the one suggested by Gueymard [18], who assumed $k_T > 0.8$, as the definition for CEE. Moreover, based on the analysis conducted herein, these two values do not depend on the particular location being analysed, and therefore they can be assumed as general constraints.

The proposed BRL-minute model was developed using CSI calculated by the broadband simplified analytical version of the Solis model [28]. This model estimates clear-sky irradiance at the evaluated site by multiplying the extraterrestrial irradiance (calculated using site latitude and longitude) by a correction factor that is a function of aerosol optical depth, atmosphere water vapor content and site altitude. The aerosol optical depth and atmospheric water-vapor content were taken from the MACC-II project database [29,30], which provides atmospheric composition data from 2003 up to 2012. However, for stations with data extending

beyond 2012, the information of the last year is used as an approximation to the atmospheric composition of the following years. This simplification has a minor impact in the proposed model as further discussed. The adoption of the broadband simplified Solis model is justified because it can be easily implemented, it is a fast algorithm and provides roughly the same level of performance as other models [31], such as McClear [32] or REST2 [33].

3. Methodology

To build the BRL-minute model the fourteen parameters β_0, β_1, …β_{13} are estimated through a least-square regression, considering measured minute data (global, diffuse and direct irradiance). The least-square procedure is fully described in Ref. [15], while the construction of a logistical separation models using minute data is described in Ref. [3]. For that purpose, two thirds of the data points were randomly selected from the set and used to determine the new β_i coefficients. The resulting correlation was then applied to the remaining third of the data to validate the model and determine the agreement through error indicators. Hence, to assess the performance of the model, irradiance data from eight radiometric stations were considered, as described in Table 1. Note that data from specified periods were used, but they are not necessary continuous.

It is worth mentioning that the separation model proposed in the present study is empirically derived from measurements, as is any other model. Therefore, the quality of the model depends on the limitation and experimental error of the measured 1-min irradiance data, in these case all three components (global, direct and diffuse irradiance) [6]. This means that the raw data should be initially filtered and validated, in order to guarantee the quality of the database, and ensuring that inconsistent and suspicious data would be removed.

3.1. Data and quality control

Recently, Lemos et al. [3] developed a robust procedure for quality control, which consists of nine steps: first filters (physical limits and solar altitude limit), plausibility check, consistency check, tracker off test, data variability test, overcast test, Rayleigh limit, clear-sky comparison and outlier removal. In the present work, the first seven steps are considered. The clear-sky comparison is unnecessary because cloud enhancements are considered in the present model. In addition, the outlier removal is not applied since the previous steps already removed most of the suspicions data. Thus, the numeric values presented in the last column *(N)* of Table 1 denote the number of points in which the three irradiance components were flagged as qualified after quality control is carried out, and used in further analysis.

3.2. Statistical indicators

Gueymard [34] presented a complete review of performance indicators that can be used in radiation models for validations purposes. Among those, four statistical indicators were considered for the formal error analysis: normalized *MAD*, normalized *RMSE*, normalized *MBE*, and the Combined Performance Index *(CPI)*, introduced in Ref. [35]. The first three indicators are classified by Gueymard [34] as Class A (indicators of dispersion), while the last one is considered Class C (indicators of cumulative distribution function (CDF) similitude). Being the *CPI* recommended in the cases where only one statistical indicator had to be selected. These indicators are defined as follows,

$$MAD = \frac{100}{\overline{d}} \frac{\left[\sum_{i=1}^{n} \left| \widehat{d}_i - d_i \right| \right]}{n} \tag{3}$$

$$RMSE = \frac{100}{\overline{d}} \sqrt{\frac{\sum_{i=1}^{n} \left(\widehat{d}_i - d_i \right)^2}{n}} \tag{4}$$

$$MBE = \frac{100}{\overline{d}} \frac{\left[\sum_{i=1}^{n} \left(\widehat{d}_i - d_i \right) \right]}{n} \tag{5}$$

$$CPI = (KSI + OVER + 2RMSE)/4 \tag{6}$$

where d_i is the actual value of the diffuse fraction calculated from measurement i, of a set of n measurements, $\widehat{d}_i$ is the estimated value of the diffuse fraction for the point i calculated using the separation model (e.g. Equation (2)), and $\overline{d}$ is the mean value of the diffuse fraction of the measurements data set. The *CPI* combines standard statistical measurements (*RMSE*) and two measurements of similarity between CDF (*KSI* and *OVER*), where the three values are expressed in percentages. The main advantage of the *CPI* is the high degree of discrimination between different models, as established in Ref. [34]. The Kolmogorov–Smirnov test Integral (*KSI*) was proposed in Ref. [36] as a measure to compute the differences between CDFs, and is expressed as follows,

$$KSI = \frac{100}{\alpha_c} \int_{x_{min}}^{x_{max}} D_n dx \tag{7}$$

where x_{min} and x_{max} are the limiting values of the independent variable, while D_n is the difference between the CDF of the measurements and the estimated values. The α_c parameter is defined as $\alpha_c = V_c(x_{max} - x_{min})$. The critical value V_c depends on the population size n and is calculated for a 99% level of confidence as $V_c =$

Table 1
Information on the eight station used for validation and creating the models.

Code	Station	Lat. (°)	Long. (°)	Elev. (m)	Source	Period	Qualified data points (N[c])
ADL	Adelaide	−34.92	138.60	50	BOM[a]	2003–2005	298,990
DAR	Darwin	−12.45	130.83	37	BOM	1999–2003	346,666
MGA	Mount Gambier	−37.83	140.78	69	BOM	1999–2005	194,662
WOO	Woomera	−31.20	136.82	169	BOM	2012–2013	178,126
FLN	Florianopolis	−27.60	−48.52	31	BSRN[b]	2013–2016	449,351
SMS	São Martinho da Serra	−29.44	−53.82	789	BSRN	2006–2014	1,185,670
BRB	Brasilia	−15.60	−47.71	574	BSRN	2004–2014	1,145,663
PTR	Petrolina	−9.06	−40.32	387	BSRN	2004–2014	932,693

[a] Australian Government Bureau of Meteorology (BOM).
[b] Baseline Surface Radiation Network (BSRN).
[c] Number of points where the three components (global, direct and diffuse irradiance) are simultaneously flagged as valid, as described in Ref. [3].

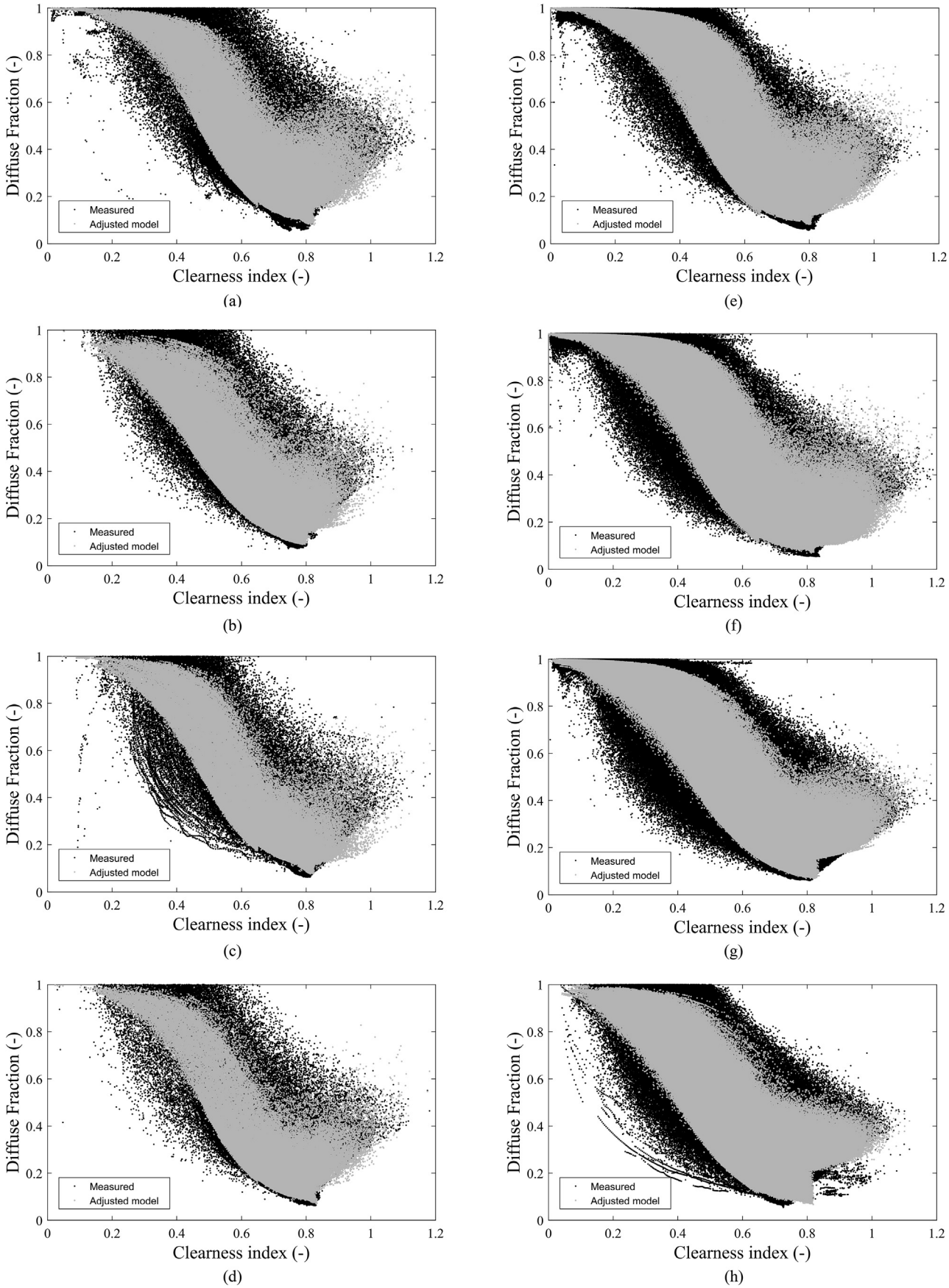

Fig. 2. Diffuse fraction data overlaid with the BRL-minute model for: (a) Adelaide, (b) Darwin, (c) Mount Gambier, (d) Woomera, (e) Florianopolis, (f) São Martinho da Serra, (g) Brasilia, and (h) Petrolina.

$1.63/\sqrt{n},\ n \geq 35$. With a KSI equal to zero the distributions are equivalent, and for larger values of KSI the model is considered non fitting to the dataset.

The *OVER* indicator was also proposed by Espinar et al. [36], which is based on the *KSI* test. *OVER* accounts for the differences between two CDFs when they exceed a critical limit (V_c), therefore, it can be calculated in percentage as follows,

$$OVER = \frac{100}{\alpha_c} \int_{x_{min}}^{x_{max}} \max(D_n - V_c, 0)dx \quad (8)$$

4. Model validation

The model was initially adjusted for each particular station to perform a graphical comparison, which is depicted in Fig. 2. As observed in the figure, the proposed model shows a good fit for the complete data set, capturing the "high clearness index – intermediate diffuse fraction" values.

Table 2 summarizes the formal error analysis of the proposed BRL-minute model and the "on-site" adjusted hourly BRL model [15] (BRL-local), for selected stations. The "on-site" BRL model is used as reference to illustrate the improvements of the proposed model. As observed in the table, the new model performs better than the reference, reducing all indicators of dispersion (Class A). Moreover, it shows significant improvements on the DNI estimations. Regarding the similitude between the distributions, both the BRL-local model and the proposed BRL-minute present almost the same *CPI* value for diffuse fraction in Florianopolis, but the BRL-minute have a significant improvement on the *CPI* value for DNI. For Adelaide, the new model also shows a significant improvement on the *CPI* value for diffuse fraction, while the DNI presents equivalent values.

Comparing Fig. 2 against the logistical format of BRL model in Fig. 1b, the new model offers a better similitude of the distributions, ratified by the indicators in Table 2. Despite the similitude of distributions, the new model is evidently better than the BRL-local model, due to the capture of cloud enhancement events (CEE), that is not reflected in the values depicted in Table 2. Those unsatisfactory results are explained by the small quantity of CEE points observed in Fig. 1a.

The site-specific models (β parameters), formal error analysis of the new model and the reference models (Ridley [15], Engerer [24], Skartveit et al. [25] and Perez et al. [4]) are provided as Supplementary Material. A closer look at the individual results in the Supplementary Material shows that new model performs significantly better than the original BRL, Engerer, Skartveit and Perez models, for both diffuse fraction and DNI, and for all stations considered herein. The new BRL-minute model shows similar dispersion indicators of the Perez model, however with a significant lower CPI. Concerning the β parameters for each station, it is also observed that they are similar enough to conclude that it is possible to create a general model for each country.

5. Results

The previous section presented further developments for the BRL model, showing its potential for modelling diffuse fraction on 1-min time scales. The present model showed significant improvements for "on-site" analysis, performing better than all other models it was compared to. The outstanding performance of the new model encourages developing a generic model suitable for more locations. However, since the number of stations considered herein is limited, it is only possible to propose generic models for Australia and Brazil.

Table 2
Error analysis for the "on-site" BRL and BRL-minute models, for Florianopolis and Adelaide.

		Florianopolis		Adelaide	
		d	DNI	d	DNI
MAD (%)	BRL local	14.92	15.23	29.53	11.42
	BRL-minute	12.56	12.22	24.51	9.19
RMSE (%)	BRL local	21.27	23.89	43.80	17.32
	BRL-minute	18.50	18.87	37.77	13.88
MBE (%)	BRL local	−1.09	3.60	−0.49	0.39
	BRL-minute	0.62	1.68	0.83	−0.27
CPI (%)	BRL local	201.41	243.17	295.43	163.59
	BRL-minute	219.95	193.27	237.16	169.61

Ridley et al. [15] developed a robust method for estimating the parameters of logistical separation models, which consists of merging the qualified data from individual stations in a single data set and submitting it to a nonlinear least-square regression. To avoid location bias in the regression, the same amount of data from each station should be considered for each country, and then subjected to the amalgamation process. After such procedure, a new set of β_i coefficients for each of Australia and Brazil was estimated, as described in the following sections.

After the development of the model using the amalgamated data of each country, the model is then applied to the data of each station separately, where a graphical performance and a formal error analysis were performed. Furthermore, the present model was compared against estimated data from well-kwon separation models. All the parameters for the different models and the results are given in the supplementary material, depicting statistical indicators, such as *KSI*, *OVER* and coefficient of determination (R^2).

5.1. Australia

The parameters estimated for Australian locations are listed in Table 3. Those values, along with Equation (2), define the Australian BRL-minute model.

A graphical comparison of the diffuse fraction and DNI estimated by Australian BRL-minute model is shown in Figs. 3 and 4, for Adelaide. The estimates delivered by the new and reference models are overlaid with actual data in a d-k_T envelop and DNI-k_T envelop. The proposed model presents a good agreement for the complete data set, as observed in Figs. 3a and 4a, and evidenced in Table 4 (detailed below). The original BRL model seems to fit the data reasonably well; however, it underestimates the diffuse fraction for high clearness index. The Engerer model also presents a good fit, capturing the shape of the data, yet it underestimates the diffuse fraction in the region where a large quantity of measurements is available ($0.5 \leq k_T \geq 0.8$). Skartveit's model seems to fit the data reasonably well, capturing all the regions of data, but it is not able to capture the overall dispersion. Finally, Perez's model also shows good fitness, nevertheless it shows sequential points, almost creating lines, featuring an unusual behaviour. Regarding the DNI estimates (Fig. 4), the BRL-minute depicts a fine adjustment to the data set, including the cloud enhancements events. The original BRL model overestimates the DNI values for high clearness index and the Engerer model seems to underestimate the DNI values over the complete data set. Finally, Skartveit's and Perez's models seem to finely capture the tendencies of the data, but similar to the other models they do not capture the dispersion.

Regarding the formal error analysis, Table 4 presents a comparison between the BRL, Engerer, Perez, Skartveit and the new

Table 3
Parameters of Equation (2) determined for Australia, hereafter known as the BRL-minute model for Australia.

β_0	β_1	β_2	β_3	β_4	β_5	β_6	β_7	β_8	β_9	β_{10}	β_{11}	β_{12}	β_{13}
−6.70407	6.99137	−0.00048	0.03839	3.36003	1.97891	−0.96758	0.15623	−4.21938	−0.00207	−0.06604	2.12613	2.56515	1.62075

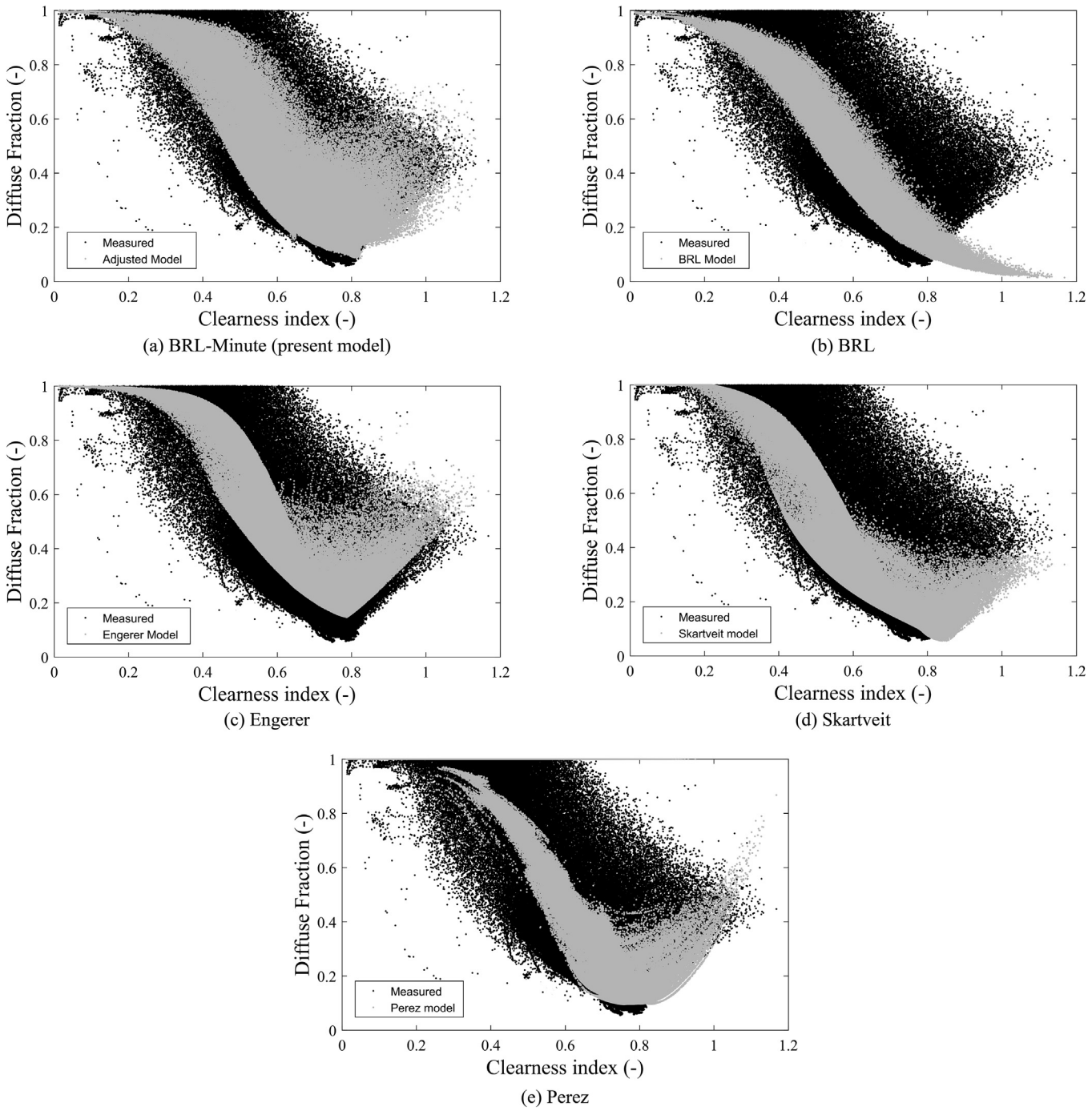

Fig. 3. Adelaide diffuse fraction data with estimates from different models overlaid.

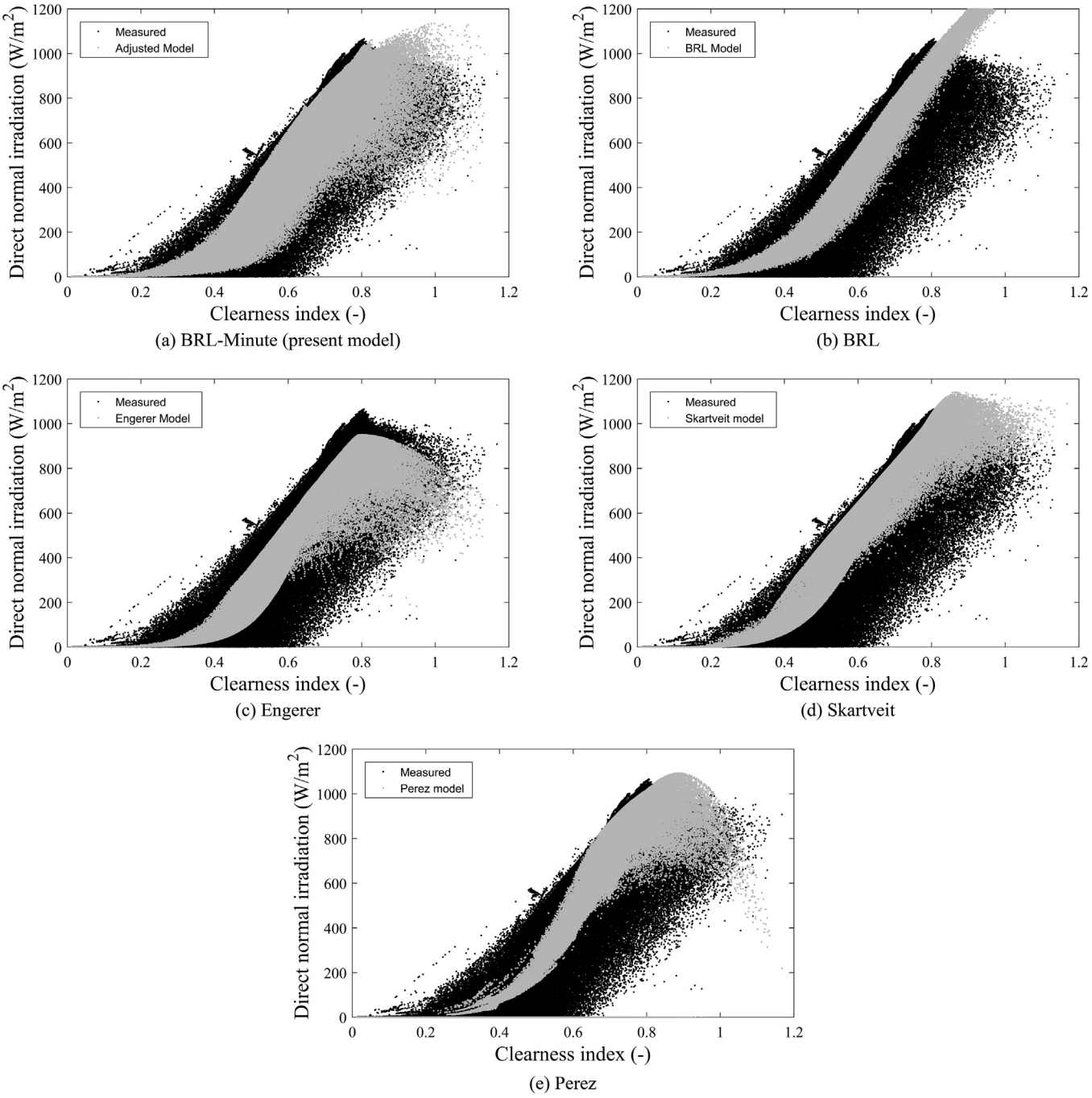

Fig. 4. Adelaide DNI data with estimates from different models overlaid.

BRL-minute models, against the actual diffuse fraction and DNI data from Australia. The performance of the models was assessed in terms of the *MAD*, *RMSE*, *MBE* and *CPI*. The results for the diffuse fraction show that the BRL-minute model performs similarly to the Perez model, and both models perform significantly better than the other ones analysed herein. However, when comparing the errors for DNI estimates, it is clearly seen that the proposed model performs better than the other models considered, showing significant improvements in similarity between distribution of data (*CPI*). Inspecting the MBE values for the BRL-minute model, it reflects a non-consistent improvement in the model performance, since some locations present a significant reduction, and others do not. One possible reason for this behaviour is due to the fact that the model was developed for a generic country, rather than a climate model, as suggested by Gueymard [6].

5.2. Brazil

The new separation model was also employed for developing a model adjusted for Brazilian conditions, where the parameters estimated are presented in Table 5. A graphical comparison in terms of diffuse fraction and DNI for Florianopolis is presented in Figs. 5 and 6, respectively. The new BRL-minute presents a fine adjustment to the complete data set, while the original BRL model

Table 4
Error analysis of diffuse fraction and DNI estimates for the Australian BRL-minute, BRL, Engerer, Perez and Skartveit models, all against the actual data for each location in Australia.

		Diffuse fraction				Direct normal Irradiance			
		Adelaide	Darwin	Mount Gambier	Woomera	Adelaide	Darwin	Mount Gambier	Woomera
MAD (%)	BRL	30.9	27.8	27.4	33.1	12.0	11.1	10.3	10.1
	Engerer	30.4	29.5	31.2	37.0	11.5	11.5	11.8	11.0
	Perez	24.6	18.8	24.0	24.2	20.9	18.6	18.4	17.4
	Skartveit	26.9	22.5	27.0	24.3	10.1	8.9	9.8	7.0
	BRL-min	25.0	20.9	24.3	24.9	9.4	8.1	8.9	7.2
RMSE (%)	BRL	45.8	35.7	41.8	48.5	18.5	14.6	16.2	15.2
	Engerer	42.2	38.6	41.5	47.3	15.5	14.5	14.8	13.6
	Perez	37.9	28.5	35.4	38.9	34.0	30.1	30.7	31.1
	Skartveit	44.8	36.4	43.5	44.4	16.9	14.8	15.5	12.9
	BRL-min	38.3	30.2	36.4	39.5	14.0	11.5	12.9	11.2
MBE (%)	BRL	−4.0	9.3	−7.3	0.2	1.88	−3.25	3.02	0.22
	Engerer	10.3	16.2	12.9	20.9	−3.90	−6.00	−5.02	−6.26
	Perez	0.9	0.1	1.3	1.4	−7.03	−9.29	−4.91	−8.57
	Skartveit	−17.6	−8.8	−18.5	−12.8	7.20	4.23	7.55	4.25
	BRL-min	0.1	5.3	−3.2	1.1	−0.02	−1.86	1.17	−0.35
CPI (%)	BRL	647.5	631.3	539.6	416.2	390.2	467.0	343.1	207.5
	Engerer	672.5	933.9	610.4	715.6	514.6	680.9	514.0	554.1
	Perez	411.4	267.2	338.8	263.7	1796.2	1220.5	1658.7	1047.9
	Skartveit	912.1	538.5	781.7	425.8	797.9	476.9	662.1	368.0
	BRL-min	424.2	350.9	394.7	310.5	302.9	233.9	270.9	203.0

Table 5
Parameters of Equation (2) determined for Brazil, hereafter known as the BRL-minute model for Brazil.

β_0	β_1	β_2	β_3	β_4	β_5	β_6	β_7	β_8	β_9	β_{10}	β_{11}	β_{12}	β_{13}
−6.37505	6.68399	0.01667	0.02552	3.32837	1.97935	−0.74116	0.19486	−3.52376	−0.00325	−0.03737	2.68761	1.60666	1.07129

underestimates the diffuse fraction and overestimates the DNI. In turn, Engerer's model overestimate the diffuse fraction, and clearly overestimates the DNI. Finally, although it appears that Skartveit's and Perez's models fit reasonably well the data, neither can capture all the dispersion of points.

Formal error analysis for Brazilian stations is presented in Table 6, in terms of the four error indicators, and comparing the results between the BRL, Engerer, Perez, Skartveit and the new BRL-minute models. As observed for the Australia model, the BRL-minute model performs similarly to the Perez model in terms of diffuse fraction, with the exception of the *MBE*, which is slightly higher than Perez's. However, for DNI estimates, the BRL-minute performs significantly better than all other models, which is depicted by all the indicators considered and for all locations analysed. It is worth mentioning that the proposed model showed notable improvements in terms of *CPI* (reducing to half for diffuse fraction and to one third for DNI), indicating high similitude between data distributions.

5.3. Influence of CSI model

Using clear-sky irradiance as a model predictor increases the complexity of the model, which is not desirable. Additionally, creating a diffuse fraction model that can only be used with a specific clear-sky model, generates a constraint that narrows the versatility of the model. The present analysis assessed the dependency of the proposed model to the model which delivers the *CSI* estimates (broadband simplified Solis clear-sky model). In that context, the impact of using different clear-sky models to evaluate the proposed minute diffuse fraction model was assessed, the aim being to verify if only the broadband simplified Solis model should be used to evaluate the BRL-minute model. For that purpose, the use of simple clear-sky models was considered, such as Perez–Ineichen [4] or Bird [37]. The inputs for the Perez-Ineichen model (i.e. Linke turbidity factor) were taken from the SoDa service [38], as described in Ref. [39]. To avoid implementation mistakes the model was downloaded from PV_LIB Toolbox [40], developed at Sandia National Laboratories. The Bird model also requires aerosol optical depth values and atmospheric water-vapor content as inputs, which were obtained from the MACC-II database, being the aerosol optical depth calculated for the specific wavelength using two values available on the database.

The BRL-minute model of each country is re-calculated for each station, but considering the clear-sky global irradiance from Bird and Ineichen-Perez, rather than the broadband simplified Solis model. Table 7 summarizes the results of this analysis for one station in Australia and Brazil, while the results for all stations are presented in the Supplementary Material.

As observed in Table 7 the different inputs delivered by the clear-sky models do not affect the *MAD* and RMSE indicators. However, they do affect the mean bias error *(MBE)* and the similitude of data distribution *(CPI)*. Yet, those differences are small, indicating that other clear-sky models could be used – recalling that more precise models should help to deliver precise results. Taking a closer look into the error indicators for all stations (supplementary material), it is possible to confirm that larger differences occur in the *MBE* and *CPI*, with slightly differences on the *MAD* and *RMSE*. Finally, itis worth mentioning that in the case of using less precise clear-sky models, it is possible to change the breakpoint of the proposed piece-wise function ($K_{CSI} \geq 1.05$) in Equation (2). This is possible because K_{CSI} is only used to classify if the event is a cloud enhancement or not. Therefore, the accuracy of the CSI models has a minor effect when using a small offset (around 1.05) for the piece-wise breakpoint.

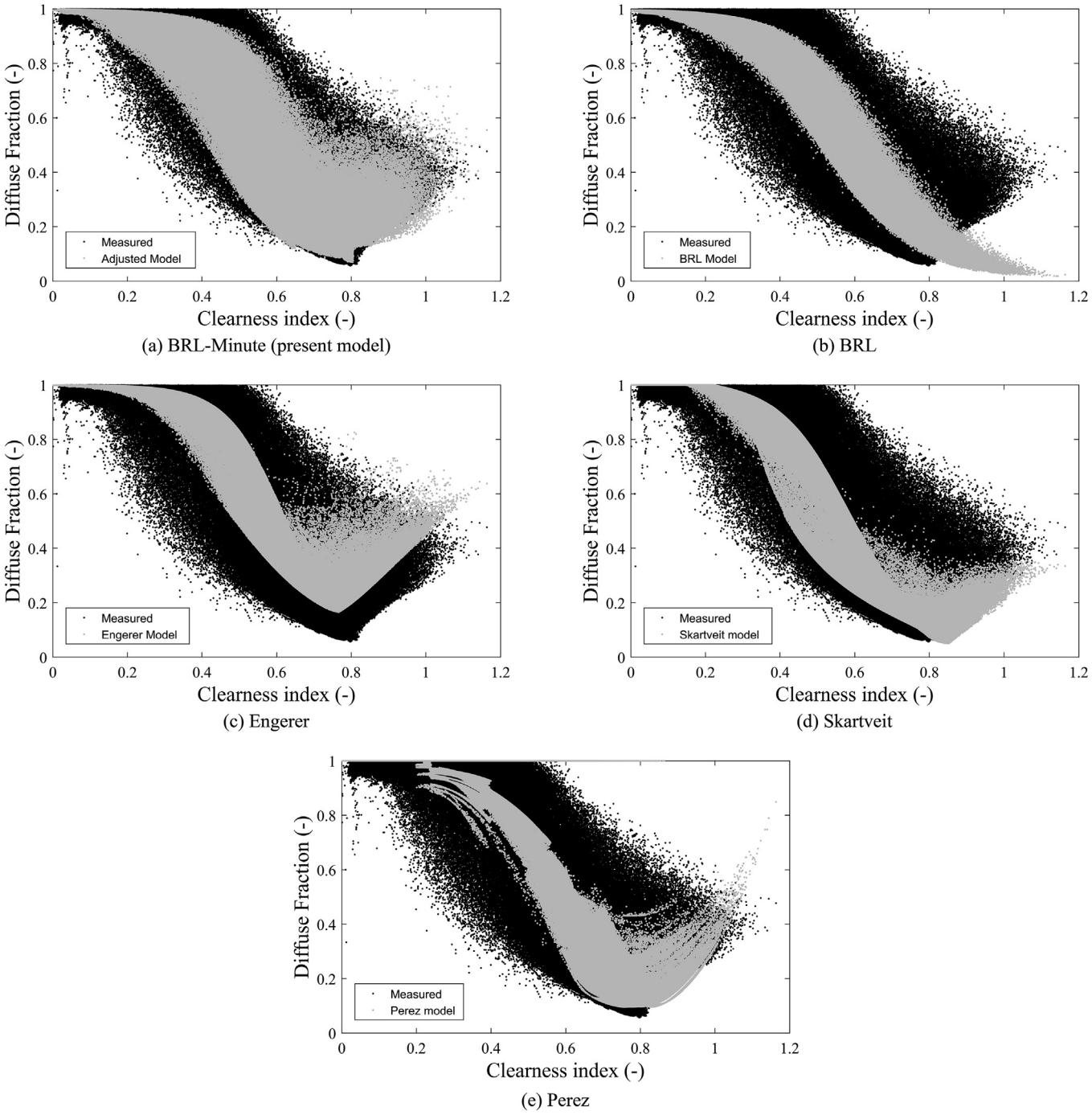

Fig. 5. Florianopolis diffuse fraction data with estimates from different models overlaid.

6. Conclusions

Accurate information about the three components of solar irradiance is fundamental for the correct design and performance assessment of solar energy systems. Yet, measuring the three irradiance components is expensive, requiring complex tracking devices and significant operational efforts. A common approach to overcome the lack of reliable information is using some sort of separation model to estimate both diffuse and direct components from global horizontal irradiance (GHI) observations. Taking these facts into consideration, the objective of this study is to derive a separation model based on a logistical function using 1-min data, which should be able to capture transient effects of irradiance, providing accurate and consistent results. To do so, we propose using a piecewise logistical function and add the clear-sky irradiance (CSI) as a predictor.

The results showed that for the “on-site” analysis, the proposed model performs better than the adjusted BRL model, capturing the cloud enhancement events (CEE). This result is evidenced analysing the KSI values for both adjusted BRL and BRL-minute models for each station (Supplementary Material), which depict reductions of up to 200%. Compared to other models, the new model performs

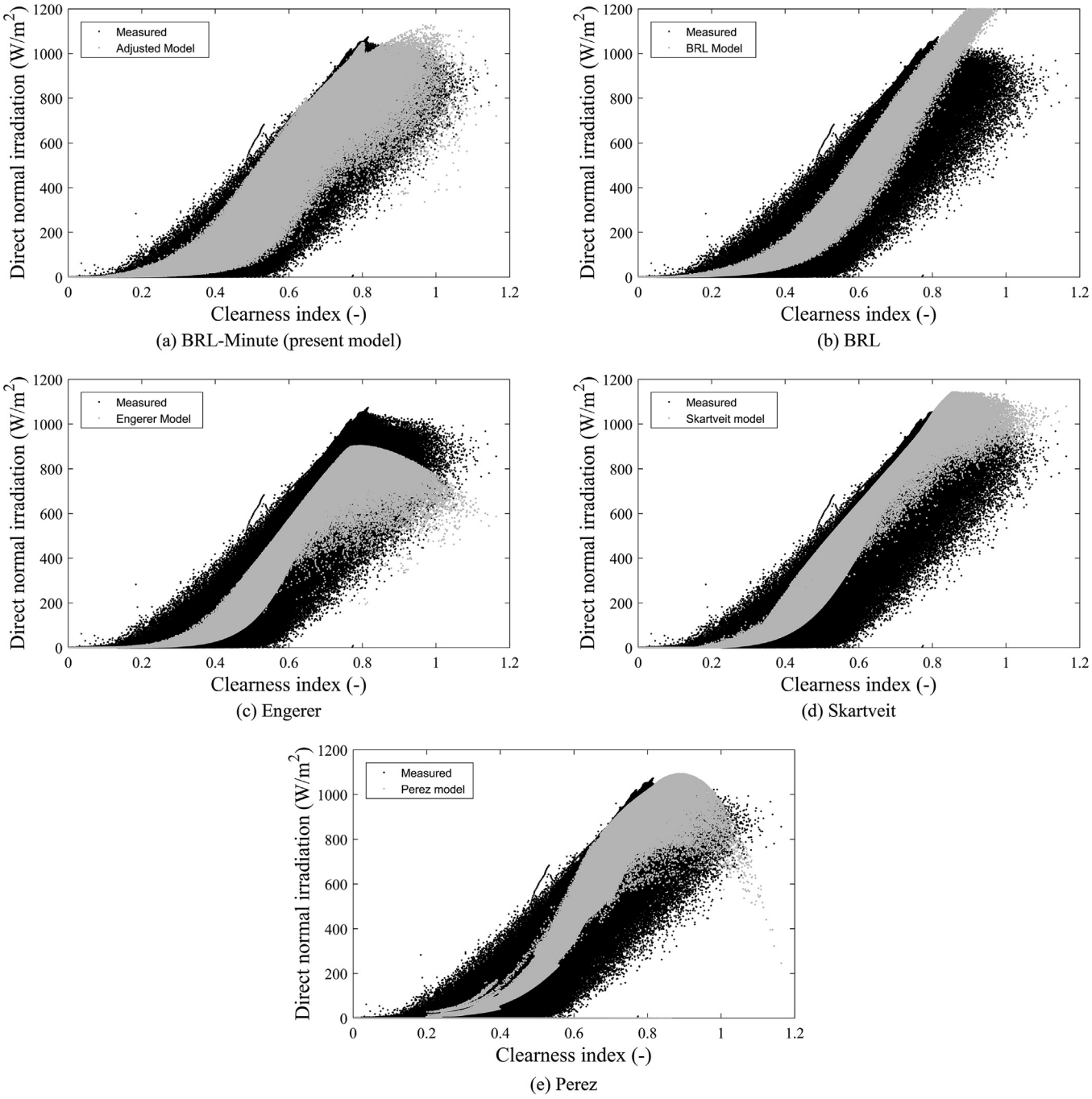

Fig. 6. Florianopolis DNI data with estimates from different models overlaid.

significantly better than the original BRL, Engerer, Skartveit and Perez models, for both diffuse fraction and DNI, and for all stations considered herein. The new BRL-minute model presents similar dispersion indicators to the Perez model, but a significantly lower CPI.

Because of the similarity between the adjusted coefficients for each station, a general model for each country, Brazil and Australia, was also proposed, and then compared against traditional models, such as: BRL, Engerer, Skartveit and Perez. The results for the diffuse fraction shows that BRL-minute model performs similarly to the Perez model, and both models perform significantly better than the other analysed herein. However, when comparing the errors for DNI estimates, it is clearly seen that the proposed model performs better than the other models considered, including the Perez model, showing significant improvements in similarity with respect to the data distribution (CPI). For Australia, the BRL-minute model (DNI estimates) performs with MAD ranging from 7 to 9%, *RMSE* from 11 to 14%, *MBE* from −2 to 2% and *CPI* from 230 to 350%. For Brazil, the BRL-minute model (DNI estimates) performs with *MAD* ranging from 10 to 13%, *RMSE* from 15 to 20%, *MBE* from −5 to 5% and *CPI* from 270 to 800%.

Finally, the influence of the clear-sky irradiance estimates on the proposed BRL-minute models is assessed. The models were built using broadband simplified Solis model, and then assessed with

Table 6
Error analysis of diffuse fraction and DNI estimates for the Brazilian BRL-minute, BRL, Engerer, Perez and Skartveit models, all against the actual data for each location in Brazil.

		Diffuse fraction				Direct normal Irradiance			
		Florianopolis	São Martinho da Serra	Brasilia	Petrolina	Florianopolis	São Martinho da Serra	Brasilia	Petrolina
MAD (%)	BRL	16.7	17.4	17.9	36.4	17.0	11.9	14.8	18.5
	Engerer	16.2	21.3	17.5	33.8	15.6	13.1	12.7	16.9
	Perez	12.6	13.0	12.9	22.5	20.9	20.5	20.0	26.7
	Skartveit	14.4	13.2	14.8	29.2	15.0	11.4	13.5	14.3
	BRL-min	13.0	13.6	12.8	25.0	12.9	10.2	11.0	12.5
RMSE (%)	BRL	22.5	23.9	24.0	43.0	25.2	19.7	22.8	21.9
	Engerer	22.4	28.2	25.6	43.4	22.5	18.6	19.2	20.6
	Perez	18.5	19.9	19.3	30.8	37.1	38.3	34.8	35.6
	Skartveit	22.0	21.8	23.1	38.1	24.6	18.9	21.8	18.2
	BRL-min	19.1	20.5	19.6	32.6	19.7	15.9	17.0	15.6
MBE (%)	BRL	−1.4	1.8	0.3	16.4	3.7	4.0	4.3	−9.8
	Engerer	6.5	14.4	10.2	21.2	−4.1	−5.9	−3.8	−11.7
	Perez	0.6	0.6	−0.5	−0.4	−1.8	−6.2	−6.3	−19.0
	Skartveit	−6.2	−2.9	−2.8	0.1	10.2	8.5	8.3	−1.6
	BRL-min	−2.6	−0.3	−1.6	6.3	4.5	5.1	5.3	−5.4
CPI (%)	BRL	534.4	815.5	772.5	1955.1	612.4	856.0	799.7	1770.9
	Engerer	751.2	2267.4	1702.0	2283.9	629.4	868.6	702.5	1796.8
	Perez	391.5	624.2	626.3	574.0	2365.9	4961.7	3841.9	1472.2
	Skartveit	777.0	642.0	978.2	720.7	1132.1	2565.5	2551.6	579.9
	BRL-min	549.5	697.7	578.9	839.0	278.0	543.6	700.6	850.5

Table 7
Error analysis of BRL-minute model considering different clear-sky models.

	Clear-sky model	Florianopolis		Adelaide	
		d	DNI	d	DNI
MAD (%)	Solis	13.0	12.9	25.0	9.4
	Bird	13.6	13.1	26.1	9.4
	Ineichen-Perez	13.2	13.8	25.9	9.6
RMSE (%)	Solis	19.1	19.7	38.3	14.0
	Bird	19.4	19.5	38.8	13.6
	Ineichen-Perez	19.5	21.6	38.9	14.2
MBE (%)	Solis	−2.6	4.5	0.1	−0.02
	Bird	−1.5	3.0	2.9	−1.2
	Ineichen-Perez	−3.2	5.8	1.4	−0.6
CPI (%)	Solis	549.5	278.0	424.2	302.9
	Bird	602.8	362.3	493.4	382.6
	Ineichen-Perez	517.3	280.7	475.3	351.3

clear-sky estimated provided by Bird and Ineichen-Perez models. The results indicate that the use of different models does not affect the *MAD* and *RMSE* indicators, but has a minor influence on the mean bias error *(MBE)* and the similitude of data distribution *(CPI)*. This is because K_{CSI} is only used to classify if the event is a cloud enhancement or not (piece-wise breakpoint). Moreover, if a less accurate CSI models is used, and it uncertainty is well known, the user can just readjust the offset of the breakpoint $(1.05K_{CSI})$.

Acknowledgments

The authors wish to express their gratitude to CAPES (Brazilian Federal Agency for Support and Evaluation of Graduate Education) for partially funding the present work through a scholarship from Allan R. Starke. The authors also appreciate the financial support from CONICYT/FONDAP 15110019 “Solar Energy Research Center”-SERC-Chile. We also thankfully appreciate the Brazilian Environmental Data Organization System (SONDA/INPE) and Australian Government Bureau of Meteorology for kindly providing the irradiance data. Finally, we also thank the MACC-II project for provide the atmospheric composition data (European project "Monitoring Atmospheric Composition and Climate - Interim Implementation" funded under the European Union's Seventh Framework Programme (FP7 THEME [SPA.2011.1.5–02]) under grant agreement n.283576).

Nomenclature

AST	Apparent Solar Time (h)
CPI	Combined Performance Index (%)
d	Diffuse fraction calculated with measured data (−)
$\widehat{d}$	Diffuse fraction calculated with model estimated data (−)
I_0	Extraterrestrial irradiance at the top of the atmosphere (W/m^2)
I_g	Global irradiance on a horizontal surface (W/m^2)
K_{CSI}	Ratio between GHI and CSI (−)
k_T	Clearness index (−)
K_T	Daily clearness index (−)
KSI	Kolmogorov-Smirnoff test Integral (%)
MAD	Mean Absolute Difference (%)
MBE	Mean Bias Error (%)
OVER	Ratio of the
RMSE	Root Mean Square Error (%)

Acronyms

BOM	Australian Government Bureau of Meteorology
BRL	Boland - Ridley - Lauret
BSRN	Baseline Surface Radiation Network
CDF	Cumulative Distribuction Function
CEE	Cloud Enhancement Event
CPV	Concentrating Photovoltaics
CSI	Clear-sky Irradiance
CSP	Concentrating Solar Power
DIF	Diffuse Horizontal Irradiance
DNI	Direct Normal Irradiance
GHI	Global Horizontal Irradiance
GTI	Global Tilted Irradiance
INMET	National Institute of Meteorology
MACC II	Monitoring Atmospheric Composition and Climate Interim Implementation
PV	Photovoltaics
SONDA	Brazilian Environmental Data Organization System
TMY	Typical Meteorological Year

Greek

α	Solar altitude angle (deg)
β	Coefficients of separation model (−)
ψ	Persistence factor (−)

Appendix A. Supplementary data

Supplementary data related to this article can be found at https://doi.org/10.1016/j.renene.2018.02.107.

References

[1] INMET, INMET Solar Stations, (n.d.). http://www.inmet.gov.br/portal/index.php?r=estacoes/estacoesAutomaticas (accessed October 26, 2017).

[2] INPE, SONDA Network, (n.d.). http://sonda.ccst.inpe.br/(accessed October 26, 2017).

[3] L.F.L. Lemos, A.R. Starke, J. Boland, J.M. Cardemil, R.D. Machado, S. Colle, Assessment of solar radiation components in Brazil using the BRL model, Renew. Energy 108 (2017), https://doi.org/10.1016/j.renene.2017.02.077.

[4] R. Perez, P. Ineichen, K. Moore, M. Kmiecik, C. Chain, R. George, F. Vignola, A new operational model for satellite-derived irradiances: description and validation, Sol. Energy 73 (2002) 307–317, https://doi.org/10.1016/S0038-092X(02)00122-6.

[5] R. Perez, T. Cebecauer, M. Súri, Semi-empirical satellite models, in: J. Kleissl (Ed.), Sol. Energy Forecast. Resour. Assess, Elsevier, 2013.

[6] C.A. Gueymard, J.A. Ruiz-Arias, Extensive worldwide validation and climate sensitivity analysis of direct irradiance predictions from 1-Min global irradiance, Sol. Energy 128 (2016) 1–30, https://doi.org/10.1016/j.solener.2015.10.010.

[7] B.Y.H. Liu, R.C. Jordan, The interrelationship and characteristic distribution of direct, diffuse and total solar radiation, Sol. Energy 4 (1960) 1–19, https://doi.org/10.1016/0038-092X(60)90062-1.

[8] R. Aler, I.M. Galván, J.A. Ruiz-Arias, C.A. Gueymard, Improving the separation of direct and diffuse solar radiation components using machine learning by gradient boosting, Sol. Energy 150 (2017) 558–569, https://doi.org/10.1016/j.solener.2017.05.018.

[9] D.T. Reindl, W.A. Beckman, J.A. Duffie, Diffuse fraction corrections, Sol. Energy 45 (1990) 1–7.

[10] J.F. Orgill, K.G.T. Hollands, Correlation equation for hourly diffuse radiation on a horizontal surface, Sol. Energy 19 (1977) 357–359, https://doi.org/10.1016/0038-092X(77)90006-8.

[11] D.G. Erbs, S.A. Klein, J.A. Duffie, Estimation of the diffuse radiation fraction for hourly, daily and monthly-average global radiation, Sol. Energy 28 (1982) 293–302, https://doi.org/10.1016/0038-092X(82)90302-4.

[12] E.L. Maxwell, A Quasi-physical Model for Converting Hourly Global to Direct Normal Insolation, 1987, pp. 35–46. http://rredc.nrel.gov/solar/pubs/PDFs/TR-215-3087.pdf.

[13] H.K. Elminir, Y.A. Azzam, F.I. Younes, Prediction of hourly and daily diffuse fraction using neural network, as compared to linear regression models, Energy 32 (2007) 1513–1523, https://doi.org/10.1016/j.energy.2006.10.010.

[14] J. Boland, B. Ridley, Models of diffuse solar fraction, Model. Sol. Radiat. Earth's Surf. Recent Adv 33 (2008) 193–219, https://doi.org/10.1007/978-3-540-77455-6_8.

[15] B. Ridley, J. Boland, P. Lauret, Modelling of diffuse solar fraction with multiple predictors, Renew. Energy 35 (2010) 478–483, https://doi.org/10.1016/j.renene.2009.07.018.

[16] J. Boland, J. Huang, B. Ridley, Decomposing global solar radiation into its direct and diffuse components, Renew. Sustain. Energy Rev. 28 (2013) 749–756, https://doi.org/10.1016/j.rser.2013.08.023.

[17] N.A. Engerer, Minute resolution estimates of the diffuse fraction of global irradiance for southeastern Australia, Sol. Energy 116 (2015) 215–237, https://doi.org/10.1016/j.solener.2015.04.012.

[18] C.A. Gueymard, Cloud and albedo enhancement impacts on solar irradiance using high-frequency measurements from thermopile and photodiode radiometers. Part 1: impacts on global horizontal irradiance, Sol. Energy 153 (2017) 755–765, https://doi.org/10.1016/j.solener.2017.05.004.

[19] C.A. Gueymard, Cloud and albedo enhancement impacts on solar irradiance using high-frequency measurements from thermopile and photodiode radiometers. Part 2: performance of separation and transposition models for global tilted irradiance, Sol. Energy 153 (2017) 766–779, https://doi.org/10.1016/j.solener.2017.04.068.

[20] T. Hirsch, H. Schenk, Dynamics of oil-based Parabolic Trough plants - a detailed transient simulation model, SolarPaces Conf (2010).

[21] T. Hirsch, H. Schenk, N. Schmidt, R. Meyer, Dynamics of oil-based Parabolic Trough plants - impact of transient behaviour on energy yields, SolarPaces Conf (2010).

[22] J. Luoma, J. Kleissl, K. Murray, Optimal inverter sizing considering cloud enhancement, Sol. Energy 86 (2012) 421–429, https://doi.org/10.1016/j.solener.2011.10.012.

[23] R.H. Inman, Y. Chu, C.F.M. Coimbra, Cloud enhancement of global horizontal irradiance in California and Hawaii, Sol. Energy 130 (2016) 128–138, https://doi.org/10.1016/j.solener.2016.02.011.

[24] N.A. Engerer, Minute resolution estimates of the diffuse fraction of global irradiance for southeastern Australia, Sol. Energy 116 (2015) 215–237, https://doi.org/10.1016/j.solener.2015.04.012.

[25] A. Skartveit, J.A. Olseth, M.E. Tuft, An hourly diffuse fraction model with correction for variability and surface albedo, Sol. Energy 63 (1998) 173–183, https://doi.org/10.1016/S0038-092X(98)00067-X.

[26] J. Boland, B. Ridley, Models of diffuse solar fraction, Renew. Energy 33 (2008) 575–584. https://doi.org/10.1016/j.renene.2007.04.012.

[27] J. a. Duffie, W.A.W.A. Beckman, Solar engineering of thermal processes, fourth ed., John Wiley & Sons, Inc, New Jersey, 2013 https://doi.org/10.1002/9781118671603.

[28] P. Ineichen, A broadband simplified version of the Solis clear sky model, Sol. Energy 82 (2008) 758–762, https://doi.org/10.1016/j.solener.2008.02.009.

[29] J.W. Kaiser, V.-H. Peuch, A. Benedetti, O. Boucher, R.J. Engelen, T. Holzer-Popp, J.-J. Morcrette, M.J. Wooster, The MACC-II management board: the pre-operational GMES atmospheric service in MACC-II and its potential usage of Sentinel-3 observations, in: Proc. 3rd MERIS/(A)ATSR OCLI-SLSTR Prep. Work., Frascati, Italy, 2012.

[30] ECMWF, MACC, Reanalysis of Global Atmospheric Composition (2003-2012), 2018. http://apps.ecmwf.int/datasets/data/macc-reanalysis/levtype=sfc/. (Accessed 19 February 2018).

[31] P. Ineichen, Validation of models that estimate the clear sky global and beam solar irradiance, Sol. Energy 132 (2016) 332–344, https://doi.org/10.1016/j.solener.2016.03.017.

[32] M. Lefèvre, A. Oumbe, P. Blanc, B. Espinar, B. Gschwind, Z. Qu, L. Wald, M. Schroedter-Homscheidt, C. Hoyer-Klick, A. Arola, A. Benedetti, J.W. Kaiser, J.J. Morcrette, McClear: a new model estimating downwelling solar radiation at ground level in clear-sky conditions, Atmos. Meas. Tech 6 (2013) 2403–2418, https://doi.org/10.5194/amt-6-2403-2013.

[33] C.A. Gueymard, Direct solar transmittance and irradiance with broadband models. Part I: detailed theoretical performance assessment, Sol. Energy 74 (2003) 355–379, https://doi.org/10.1016/j.solener.2003.11.002.

[34] C.A. Gueymard, A review of validation methodologies and statistical performance indicators for modeled solar radiation data: towards a better bankability of solar projects, Renew. Sustain. Energy Rev. 39 (2014) 1024–1034, https://doi.org/10.1016/j.rser.2014.07.117.

[35] C.A. Gueymard, Clear-sky irradiance predictions for solar resource mapping and large-scale applications : improved validation methodology and detailed performance analysis of 18 broadband radiative models, Sol. Energy 86 (2012) 2145–2169, https://doi.org/10.1016/j.solener.2011.11.011.

[36] B. Espinar, L. Ramírez, A. Drews, H.G. Beyer, L.F. Zarzalejo, J. Polo, L. Martín, Analysis of different comparison parameters applied to solar radiation data from satellite and German radiometric stations, Sol. Energy 83 (2009) 118–125, https://doi.org/10.1016/j.solener.2008.07.009.

[37] R. Bird, R.L. Hulstrom, Simplified clear sky model for direct and diffuse insolation on horizontal surfaces, 1981, https://doi.org/10.2172/6510849. Golden, CO (USA).

[38] SoDa Service, 2017. http://www.soda-pro.com/web-services/atmosphere/turbidity-linke-2003. (Accessed 1 January 2017).

[39] J. Remund, L. Wald, M. Lef, T. Ranchin, J. Page, Worldwide Linke turbidity information, in: Proc. ISES Sol. World Congr. 2003, Inter- national Solar Energy Society (ISES), Goteborg, Sweden, 2003, p. 13.

[40] Sandia National Laboratories, PV_LIB Toolbox - Pvl_clearsky_ineichen, 2017. https://pvpmc.sandia.gov/applications/pv_lib-toolbox/. (Accessed 1 January 2017).